Title

Multiparameter evaluation of in vivo gene delivery using ultrasound-guided, microbubble-enhanced sonoporation

Authors

Shapiro, Galina
Wong, Andrew W
Bez, Maxim
et al.

Publication Date

2016-02-01

DOI

10.1016/j.jconrel.2015.12.001

Peer reviewed

HHS Public Access

Author manuscript

J Control Release. Author manuscript; available in PMC 2017 February 10.

Published in final edited form as:

J Control Release. 2016 February 10; 223: 157–164. doi:10.1016/j.jconrel.2015.12.001.

Multiparameter evaluation of in vivo gene delivery using ultrasound-guided, microbubble-enhanced sonoporation

Galina Shapiro[a,*], **Andrew Wong**[b,*], **Maxim Bez**[a], **Fang Yang**[b], **Sarah Tam**[b], **Lisa Even**[b], **Dmitriy Sheyn**[c,d], **Shiran Ben-David**[c,d], **Wafa Tawackoli**[c,d,e], **Gadi Pelled**[a,d,e], **Katherine W. Ferrara**[b,#], and **Dan Gazit**[a,d,e,#]

[a]Skeletal Biotech Laboratory, The Hebrew University–Hadassah Faculty of Dental Medicine, Ein Kerem, Jerusalem 91120, Israel

[b]University of California, Davis, Department of Biomedical Engineering, 451 Health Sciences Drive, Davis, CA 95616, USA

[c]Department of Surgery, Cedars-Sinai Medical Center, 8700 Beverly Blvd., Los Angeles, CA 90048, USA

[d]Board of Governors Regenerative Medicine Institute, Cedars-Sinai Medical Center, Los Angeles, CA 90048, USA

[e]Biomedical Imaging Research Institute, Cedars-Sinai Medical Center, Los Angeles, CA 90048, USA

Abstract

More than 1800 gene therapy clinical trials worldwide have targeted a wide range of conditions including cancer, cardiovascular diseases, and monogenic diseases. Biological (i.e. viral), chemical, and physical approaches have been developed to deliver nucleic acids into cells. Although viral vectors offer the greatest efficiency, they also raise major safety concerns including carcinogenesis and immunogenicity. The goal of microbubble-mediated sonoporation is to enhance the uptake of drugs and nucleic acids. Insonation of microbubbles is thought to facilitate two mechanisms for enhanced uptake: first, deflection of the cell membrane inducing endocytotic uptake, and second, microbubble jetting inducing the formation of pores in the cell membrane. We hypothesized that ultrasound could be used to guide local microbubble-enhanced sonoporation of a reporter gene encoding DNA. With the aim of optimizing delivery efficiency, we used nonlinear ultrasound and bioluminescence imaging modes to optimize the acoustic pressure, microbubble concentration, treatment duration, DNA dosage, and number of treatments required for *in vivo Luciferase* gene expression in a mouse thigh muscle model. We found that mice injected with 50

Correspondence should be addressed to Dan Gazit (Dan.Gazit@csmc.edu) Dan Gazit, DMD, PhD Skeletal Regeneration and Stem Cell Therapy Program Molecular & Micro Imaging Core Department of Surgery The Board of Governors Regenerative Medicine Institute (RMI) Cedars- Sinai Medical Center AHSP, Rm A8108 8700 Beverly Blvd. Los Angeles, CA 90048. Tel: Office 310-248-8575, lab 310-248-8562.

*Equal contribution.

#Equal senior contribution.

μg luciferase plasmid DNA and 5 x 105 microbubbles followed by ultrasound treatment at 1.4 MHz, 200 kPa, 100-cycle pulse length, and 540-Hz pulse repetition frequency (PRF) for 2 min exhibited superior transgene expression compared to all other treatment groups. The bioluminescent signal measured for these mice on Day 4 post-treatment was 100-fold higher ($p < 0.0001$, $n = 5$ or 6) than the signals for controls treated with DNA injection alone, DNA and microbubble injection, or DNA injection and ultrasound treatment. Our results indicate that these conditions result in efficient gene delivery and prolonged gene expression (up to 21 days) with no evidence of tissue damage or off-target delivery. We believe that these promising results bear great promise for the development of microbubble-enhanced sonoporation–induced gene therapies.

Graphical abstract

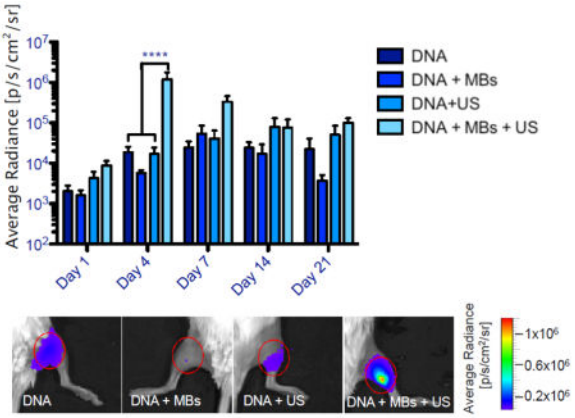

Keywords

"Ultrasound"; "Microbubbles"; "Sonoporation"; "Gene therapy"

Introduction

Gene-based therapy is the modulation of gene expression intended to prevent, stop, or reverse a pathological process. Therapeutic exogenous nucleic acids, such as DNA, mRNA, microRNA, and small interfering RNA, are used to change gene expression. More than 1800 gene therapy clinical trials worldwide have targeted a wide range of pathologies, including cardiovascular and monogenic diseases [1]. The most commonly transferred gene types are antigens, cytokines, and tumor suppressors to treat cancer. Regenerative medicine – oriented gene therapy approaches have also been investigated for the treatment of many diverse conditions such as β-thalassemia, rheumatoid arthritis, myocardial infarction, and Duchenne muscular dystrophy [1].

While gene therapy has many possible applications, developing effective and safe delivery vectors remains a major challenge. Since both nucleic acids and the cell membrane are negatively charged, electrostatic forces result in their mutual repulsion. To overcome this limitation, biological (i.e. viral), chemical, and physical approaches have been developed.

Although viral vectors are the most efficient and commonly used vectors applied in clinical trials, their use raises major concerns such as carcinogenesis [2], immunogenicity [3], off-target delivery [4], and difficulty of vector production [5]. Nonviral gene therapy could potentially address many of these safety limitations, mostly at the expense of lower efficiency of gene delivery. Nonviral approaches include the injection of naked DNA alone or via physical methods such as electroporation, sonoporation, and magnetofection [6–8].

Sonoporation is the use of ultrasound to increase cell membrane permeability, thus enhancing uptake of drugs and nucleic acids [9, 10]. A mechanical method, sonoporation induces a spatiotemporally controlled, transient formation of pores in the cell membrane, which is followed by restoration of cell membrane integrity. Since ultrasound application can be localized to a region of interest, deep tissues can be specifically sonoporated with minimal systemic effects. Most sonoporation studies have combined plasmid DNA with microbubbles (MBs) in order to enhance membrane permeability via the effects of microbubble volume fluctuations and/or collapse [11–15]. The mechanisms for microbubble-mediated sonoporation depend on acoustic pressure [16–18]. At low-pressure amplitudes, microbubbles decrease and increase in size successively, subsequently pushing and pulling adjacent cell membranes [16, 17]. At the same time, the ultrasonic radiation force initiates motion and displacement of the oscillating microbubbles. The movement of oscillating microbubbles causes cell membrane deformation, which is hypothesized to induce endocytosis [18, 19]. At high-pressure amplitudes and low ultrasound frequencies, microbubbles will rapidly collapse, producing liquid jets capable of penetrating cell membranes and creating microstreaming, shock waves, and shear stresses [20, 21]. In addition, microbubbles can reach extremely high pressures and temperatures, resulting in friction that can create pores in the cell membrane [22].

In addition to enhancing sonoporation, microbubbles can serve as imaging contrast agents [23]. They are composed of a gas core and a stabilizing shell, which is usually composed of lipids, proteins, or polymers. Since the average diameter of microbubbles is 1–10 μm, they can be safely injected systemically and used to image vascular structures. The gas core reflects and scatters the ultrasound field, thereby increasing contrast between the vasculature and surrounding tissue. Recent advances have allowed researchers to functionalize microbubbles to carry a payload and/or to specifically target desired cell populations [24]. Nevertheless, microbubblemediated sonoporation remains a complex strategy involving microbubble excitation by ultrasound, excited microbubble-cell interactions, intracellular delivery of nucleic acids, and gene expression modulation. Here, we use the contrast-pulse sequencing (CPS) imaging mode to optimize the insonation parameters with a goal of visualizing the oscillation of the injected microbubbles over a period of minutes. As compared to systemically injected microbubbles, which will continuously replenish a region, local therapies require an approach in which microbubbles are not immediately destroyed, but instead stably transfect cells. Taking advantage of the minimally invasive, local, and targeted nature of sonoporation while optimizing delivery efficiency and minimizing side effects will be key to advancing sonoporation to the clinic.

Previous studies have not comprehensively optimized the various parameters involved in local microbubble-assisted sonoporation for *in vivo* gene delivery. In the present study we

compared *in vivo* reporter gene expression over time between mice treated with different combinations of various doses of DNA and microbubbles, acoustic pressures, treatment durations, and numbers of treatments. The aim of the present study was to pave the way to development of efficient nonviral gene therapy for regenerative medicine.

Methods

Ethics Statement

All animal experiments were performed under a protocol approved by the Institutional Animal Care and Use Committee (IACUC) of the University of California, Davis (Protocol No. 17336). Anesthesia was administered for all imaging and surgical procedures. All mice were housed in accordance with approved IACUC protocols.

Plasmid DNA production

The reporter vector pLuc2 encoding for the *luciferase2* gene under the control of the ubiquitin promoter was used to monitor transgene expression in vivo. The plasmid was amplified using standard procedures and purified using an EndoFree Kit (Qiagen, Valencia, CA, USA).

Microbubble production

Phospholipids were purchased from Avanti Polar Lipids (Alabaster, AL, USA). Microbubbles were prepared as described previously [25]. Briefly, 1,2-dipalmitoyl-*sn*glycero- 3-phosphocholine, 1,2-dipalmitoyl-*sn*-glycero-3-phosphate, and 1,2- dipalmitoyl-*sn*-glycero-3-phosphoethanolamine-N-[methoxy(polyethylene glycol)- 5000] in a 0.82/0.1/0.08 molar ratio were rehydrated with a degassed buffer of normal saline, propylene glycol, and glycerol in a 0.8/0.1/0.1 v/v/v ratio and adjusted to a pH of 7.2–7.4 for a total concentration of 2.5 mg of lipid per 1 ml buffer. This solution was transferred to a vial, and the headspace of the vial was replaced with perfluorobutane. Lipid suspension was activated by 45 sec of shaking within a Vialmix shaker (Lantheus Medical, N. Billerica, MA, USA). Following activation, the bubbles were washed three times with Dulbecco's phosphate-buffered saline (DPBS, Thermo Fisher Scientific) without calcium or magnesium, and a bubble cake was formed by gentle centrifugation for 3 min at 1000 RPM in a Centra CL2 centrifuge (Thermo Fisher Scientific Inc., Waltham, MA, USA). The buffer solution was discarded and replaced with fresh DPBS. The bubble cake was then gently inverted to mix. Following washing, the bubbles were sized with an Accusizer 770A unit (Particle Sizing Systems, Port Richey, FL, USA) and used within 3 hours.

Spacer production

Agarose powder (Avocado Research Chemicals, Morecambe, UK) and DPBS were combined in a weight/total-volume ratio of 2%. They were mixed and microwaved until completely dissolved (90°C) and then placed in a vacuum for 10 min for degassing. After degassing, the solution was poured into a cubic mold and allowed to solidify for at least 3 h at room temperature (23°C). Finally, the spacer was cut down to 3 cm x 5 cm x 3.25 cm to fit the ultrasound transducer and allow for treatment at the natural focus of the ultrasound beam.

Ultrasound setup

In this study, we used a Siemens Antares system (Siemens Health Care, Inc., Ultrasound Division, Mountain View, CA, USA) with software modifications; a custom array transducer, known as a co-linear array and described elsewhere [26]; a control system; and a feedback path into the scanner. Images were acquired using the Cadence Contrast Agent Imaging mode (also known as CPS) at 5.33 MHz. For the transfection studies, we used the following parameters: 1.4 MHz, 100-cycle pulse length, 540-Hz PRF, with the CPS imaging frame acquired every second. The transducer was set to face upward, allowing the spacer to be attached to it using ultrasound gel (Aquasonic, Parker Laboratories, Fairfield, NJ, USA) to couple them. On top of the spacer more ultrasound gel was used to couple the mouse thigh to the spacer.

Parameter optimization

An initial in vitro study was performed to determine the approximate parameter range for the ultrasound pressure and microbubble concentration. In this study, microbubbles were injected into a saline-filled void in an agarose gel spacer. Parameters that resulted in a visible CPS image for a period of at least 2 minutes were selected for testing in vivo.

In vivo gene delivery

Female FVB/N mice (10 wks old, Charles River, Wilmington, MA, USA) were anesthetized by continuous administration of 1%–3% isoflurane mixed with 100% medical-grade oxygen, after which the animals were shaved to remove all fur from both thighs. The thigh of interest was swabbed with 70% ethanol and placed in ultrasound gel on the spacer (Fig. 1B,C). Finally, the thigh was covered with more ultrasound gel to reduce reflections.

Using ultrasound guidance, we injected either plasmid DNA or a mixture of plasmid DNA and microbubbles into the thigh muscle, close to the femur (Fig. 1E; see Table 1 for the various treatment groups). Specifically, between 25 μg and 100 μg plasmid DNA was premixed with between 5 x 104 and 5 x 106 microbubbles per 20 μl or PBS. A total volume of 20 μl per injection was kept constant for all the studies and the injection was performed at a consistent rate, requiring approximately 5 seconds to inject the entire volume. Immediately after the injection, the needle was removed and the therapeutic ultrasound sequence was applied to some animals (Fig. 1F). Different sequences were tested by varying the amplitude between 50 kPa and 320 kPa as well as the total treatment time between 0.5 min and 10 min. During treatment, the injection site was visualized using CPS imaging. Finally, the injection and the ultrasound sequence were repeated for some animals for a total of two treatments. After both thighs had been treated, the mouse was allowed to recover in a warmed cage.

Bioluminescence imaging

Luciferase expression in the thigh muscle was detected and recorded at different time points using a BLI system, as described previously [27, 28]. Briefly, 10 min before BLI of the mice commenced, the animals were given an intraperitoneal injection of luciferin diluted with PBS (126 mg/kg body weight; Promega, Madison, WI, USA). Then the mice were anesthetized by continuous administration of 1.0%–3.0% isoflurane mixed with 100% medical-grade oxygen. Light emission was evaluated using the IVIS Spectrum system

(Perkin Elmer, Waltham, MA, USA). The exposure time was set automatically, and bioluminescence was quantified as the average signal normalized to the exposure time and the area covered by the region of interest. Bioluminescence for each animal was measured on Days 1, 4, 7, 14, and 21 after treatment (Day 0).

Histological and immunofluorescence analyses of reporter gene expression

To analyze muscle tissue after the various treatments and to detect luciferaseexpressing cells, four mice (one per group, groups 3, 18–20) were sacrificed 21 days after treatment. Hind limbs were removed and processed for histological analysis, as previously described [28]. Briefly, tissue samples were fixed in 4% formalin, decalcified using 0.5M Ethylenediaminetetraacetic acid solution (EDTA, pH 7.4), dehydrated using a graded series of ethanol solutions, and embedded in paraffin. Sections (5 μm thick) were cut from each paraffin block using a motorized microtome (Leica Microsystems, Wetzlar, Germany). Hematoxylin and eosin (H&E) staining was performed to evaluate the morphological characteristics of the tissue. To detect cells that had been transfected with the reporter gene, immunofluorescent staining against the luciferase (Luc) protein was carried out. Slides were deparaffinized, and the antigens were retrieved by incubation in preheated Target Retrieval SolutionTM (Dako, Carpinteria, CA) for 45 min in 37°C. Nonspecific antigens were blocked by applying blocking serum – free solution (Dako, Carpinteria, CA). The slides were incubated with primary rabbit anti-luciferase polyclonal antibody (diluted in PBS at a ratio of 1:250, Cortex Biochem, San Leandro, CA) overnight in 4°C and with secondary Alexa Fluor® 488-conjugated donkey anti-rabbit antibody (diluted in PBS at a ratio of 1:1000, Jackson ImmunoResearch Laboratories, West Grove, PA) for 1 h at room temperature, after which the slides were washed with PBS. The slides were then stained with 4',6-diamidino-2-phenylindole dihydrochloride (DAPI, 1 μg/ml) for 5 min in the dark, after which they were again washed three times with PBS. VectaMountTM mounting medium (Vector Laboratories, Burlingame, CA) was applied to the tissue. Photomicrographs were obtained using a four-channel Laser Scanning Microscope 780 (Zeiss, Pleasanton, CA) with 20× magnification, z-stacking, and 2 x 2 tile scanning. All samples were scanned using the same gain and exposure settings.

Statistical analysis

Values are expressed as mean and standard error. Longitudinal data analysis was conducted to compare gene expression between treatments by performing two-way analysis of variance with Bonferroni post-tests using GraphPad Prism, version 5.00 for Windows (GraphPad Software, San Diego CA, USA, www.graphpad.com).

Results

Acoustic pressure effect

All treatment protocols resulted in a visible CPS image within the muscle for approximately 1.5 minutes. Further, all treatment protocols resulted in well-localized transient gene expression with maximal expression on Days 4 and 7 post-treatment. The bioluminescence intensity measured for the 200 kPa group (Group 3) was significantly higher on Day 4 (100-fold, $p < 0.01$) than the 50 kPa treatment group (Group 1) and more than 10-fold higher than

the 100 kPa, 250 kPa, and 320 kPa groups (Groups 2, 4, and 5, respectively) (Fig. 2). Luciferase expression decreased over time after Day 4, until no signal was detected on Day 21 in all but one group: the 200 kPa group (Group 3). Luciferase expression for the 200 kPa group was found to last until Day 42 (data not shown).

Microbubble dose effect

Almost all treatment groups exhibited well-localized transient gene expression with peak expression on Days 4 and 7; the exception was the 5 x 106 microbubble treatment group (Group 9), for which low-to-no expression of luciferase was found at all time points (Fig. 3). The 5 x 105 microbubble treatment group (Group 3) exhibited significantly higher transfection efficiency (100-fold, $p < 0.0001$) than all other groups on Day 4.

Treatment time effect

When the total treatment time was increased from 0.5 min (Group 10) to 2 min (Group 3), we detected significantly increased efficiency of gene transfection on Days 4 ($p < 0.001$) and 7 ($p < 0.05$) (Fig. 4). However, no increase in gene delivery efficiency was observed for longer treatment times, such as 3 min (Group 12) and 10 min (Group 13) ($p > 0.05$ for a comparison of Groups 12 and 13).

DNA dose and the multiple treatment effect

Animals treated with 50 μg pLuc2 once (Group 3, “50 ug once”) demonstrated significantly greater gene expression than animals treated with 25 μg once (Group 14, “25 ug once”) or 100 μg once (Group 17, “100 ug once”) pLuc2 when examined on Days 4 ($p < 0.05$) and 7 ($p < 0.05$) post-treatment (Fig. 5). Interestingly, pLuc2 treatment at a dose of 25 μg once (Group 14) or 100 μg once (Group 17) resulted in the same luciferase activity at all time points.

In addition to investigating whether increasing the DNA concentration would increase transfection efficiency, we also looked into the possible use of repeated treatments to improve gene delivery. Two groups of mice were treated with two consecutive injections of 5 x 105 microbubbles and 25 μg pLuc2 (Group 15, “25 ug twice”) or 5 x 105 microbubbles and 50 μg pLuc2 (Group 16, “50 ug twice”), providing total amounts of 50 μg and 100 μg DNA, respectively. Therapeutic ultrasound with an acoustic pressure of 200 kPa was applied for 2 min after each mixture injection. Both treatment regimens resulted in significantly lower luciferase activity than that found in 50 μg once group on Day 4 (Fig. 5, $p < 0.05$).

Combining ultrasound and microbubbles for gene delivery

After individually optimizing the acoustic pressure, the duration of ultrasound application, and the dosage of microbubbles and DNA for gene delivery, we compared the optimized treatment (protocol used in Group 3) to the results obtained in the control groups (Groups 18 – 20). The following controls were used: DNA injection alone (Group 18, “DNA”); injection of both DNA and MBs (Group 19, “DNA + MBs”); and injection of DNA with ultrasound (US) treatment (Group 20, “DNA + US”). Only the combined DNA-microbubble injection followed by ultrasound treatment (Group 3, “DNA + MBs + US”) resulted in a 100-fold significant increase ($p < 0.0001$) in luciferase activity on Day 4 compared to all controls

(Fig. 6A). Furthermore, immunofluorescence analysis (Fig. 7) demonstrated significantly more *Luciferase* expression on Day 21 for the DNA + MBs + US group compared to gene expression in the control groups. Importantly, no evidence of structural damage to muscle or bone was found for the optimized treatment group or controls (H&E staining, Fig. 7). In conclusion, the optimized DNA + MBs + US group was found to result in an early (Days 4 and 7, Fig. 6A) and lasting (Day 21, Fig. 7) significant increase in gene delivery efficiency while keeping up with a spatial (Fig. 6B – E) and temporal (H&E, Fig. 7) expression pattern that is consistent with nonviral gene delivery systems.

Discussion

Ultrasound is widely used in the clinic for diverse purposes such as imaging, lithotripsy, and tumor ablation. Preclinical studies have been conducted to investigate the possibility of ultrasound-mediated gene therapy. This is an attractive approach, because it results in transient gene expression and does not require potentially tumorigenic and immunogenic viral vectors or invasive electroporation. However, the major limitation of ultrasound-mediated gene delivery is its relatively lower efficiency compared to the aforementioned methods. Therefore, optimizing the efficiency of ultrasound-mediated gene delivery is crucial in promoting its future therapeutic applicability.

In this study, we explored a number of key parameters affecting local naked DNA delivery by using microbubble-assisted sonoporation. First, we looked at the effect of acoustic pressure on delivery efficiency. Low acoustic pressures are known to induce symmetrical microbubble oscillations, known as stable cavitation, with microbubble oscillations deflecting the cell membrane and potentially inducing endocytotic uptake. Higher acoustic pressures cause rapid growth of microbubbles and inertial cavitation. Shock waves and microjets produced by inertial cavitation are very stressful for cell membranes, resulting in membrane disruption and perforation [29]. As a result, the effects of inertial cavitation extend further into the tissue. Our study shows that increasing the acoustic pressure from 50 kPa to 250 kPa increases gene expression on Day 4 to the maximum and that no further increases in gene expression result from higher pressures. The reduction in gene expression at higher pressures may be a result of increased cell lysis and apoptosis [30, 31]. Since bioluminescence imaging was used to measure gene expression its limitations may have also influenced these results. While bioluminescence imaging is very common, highly sensitive and specific the complexity of the luciferase catalyzed reaction and *in vivo* light propagation pose certain limitations. Regarding the luciferase-luciferin reaction both substrate and co-factors: ATP, oxygen and magnesium are required so limited availability of any of these components may result in an underestimation of luciferase activity [32]. Additional factors influencing luciferase activity include pH, perfusion and cellular viability [33]. While the aforementioned factors could have been modified by the change in treatment we have found a strong correlation between in vivo bioluminescence signal (Fig. 6) and *ex vivo* immunohistochemical staining for luciferase expression (Fig. 7).

It is also important to recognize that each treatment involved only a single injection of microbubbles and the higher acoustic pressure rapidly destroyed the microbubble population. The limited microbubble lifetime in the face of higher acoustic pressure may

also play a role in the decrease in observed transfection. Therefore, to achieve maximal gene delivery efficiency, one must apply enough acoustic pressure to excite microbubbles but not irreversibly damage the cells or immediately destroy the microbubbles. Avoiding cell damage is particularly important for regenerative purposes. Interestingly, the optimal acoustic pressure found in this study was lower than acoustic pressures reported in some similar studies [11, 34]. Although no structural damage was reported in those studies, our results indicate that even lower acoustic pressures may be used for successful gene delivery, so the probability of side effects such as tissue heating would be reduced, thereby providing a safer delivery protocol.

Next we found that delivery of 5 x 105 microbubbles per 50 μg DNA led to significantly enhanced transfection when compared to lower and higher dosages of microbubbles. This result suggests that the concentration of microbubbles in the injected solution must be kept in a very tight range to achieve enhanced sonoporation. Below this concentration, there may be too little impact from microbubble oscillation and the microbubbles may be more rapidly destroyed. If the microbubble concentration is too high, however, the microbubbles may shield each other from the acoustic field and the effect would be attenuated. Alternatively, too many microbubbles could cause increased tissue damage. Previous studies reported using higher concentrations of injected microbubbles for intramuscular gene delivery [35, 36]. For example, Li et al. [36] used as many as 8 x 106 microbubbles per 20 μl (Sonidel MB101®, Sonidel Ltd, Ireland), which were similar in size and structure to the microbubbles used in our study for sonoporation in the mouse hind leg muscle. However, since no data on gene expression without ultrasound treatment were shown, it is hard to conclude whether such a high concentration of microbubbles can effectively enhance sonoporation.

Similar to our results, Nomikou et al. [37] found that higher microbubble concentrations significantly reduced cell viability but did not increase transfection efficiency. We found that prolonged ultrasound exposure (> 2 min, Fig 5) and excess DNA (> 50 μg) decrease the efficiency of gene transfection. Both prolonged ultrasound exposure and excess DNA can also result in cellular toxicity via a mechanical mechanism [38]. Here, optimized ultrasound exposure time and microbubble concentration correlated with microbubble survival observed by CPS imaging. Nonlinear contrast imaging of microbubbles may be a useful approach to maximize transfection while minimizing cellular toxicity in other tissue types. Delalande et al. [39] evaluated the effect of different parameters on gene expression in the Achilles tendon of mice. While similar ultrasound settings and microbubble concentrations were found to be optimal by that group, their total treatment time was 10 min compared to our 2 min. This probably stems from differences in the acoustic properties surrounding the region of interest. The Achilles tendon, being closer to bone than the thigh muscle, is a more difficult site for sonoporation because bone is highly reflective of ultrasound waves. Therefore, it is very likely that a longer treatment time is needed to induce the same treatment effect in tendon that is observed in muscle.

Another important factor is the microbubble shell, which can be composed of either a lipid or a protein. Different shell structures behave differently when ultrasound is applied. Protein-shelled microbubbles have a thicker and more rigid shell [40]. In contrast, lipid

shells are held together by “weak” forces, which make them more compliant to expansion and compression during ultrasound sonication. Lipid shells also possess the ability to reseal themselves following fragmentation [41]. Therefore, lipid-shelled microbubbles exhibit favorable characteristics for ultrasound-mediated gene delivery. In one report, commercially available lipid shells (Definity, Lantheus Medical, N. Billerica, MA, USA) were associated with higher efficiencies related to uptake of DNA and different drugs than protein-shelled microbubbles (Optison, GE Healthcare, Princeton, NJ, USA) [42].

One of the parameters not tested in this study is the effect of microbubble size and composition on gene delivery. Previous studies showed that cavitation behavior and stability of microbubbles mainly depend on microbubble size [43, 44]. The natural frequency of microbubbles depends on their diameter [45]. Also, large microbubbles are known to be more resistant to destruction and can require higher acoustic pressures to achieve the same wall velocity and therefore affect membrane permeability. For the study performed here, the persistence of the small microbubbles was sufficient to achieve transfection. In other applications, larger microbubbles may be desired to extend the oscillation lifetime. An additional factor that could increase the transfection efficiency is the use of lipoplexed DNA that is shielded from nucleases. Future studies should also explore the possibility of using lipoplexed DNA for pre clinical and clinical trials.

In this study, we used the CPS image to monitor microbubble oscillation. CPS image amplitude is dependent on nonlinear microbubble oscillation and therefore can be used to monitor microbubble persistence. With the Antares system used in this study, specific harmonics could not be differentiated and therefore the nature of the cavitation (transient or stable) was assessed only by the microbubble lifetime. Future studies will emphasize the development of capabilities to directly assess cavitation.

These results bear great promise for the future development of therapies based on direct gene delivery to tissues. Our data clearly demonstrate that ultrasoundmediated gene delivery is dependent on acoustic pressure, microbubble and DNA dosage, and treatment time. The combination of these parameters allows an efficient and prolonged gene expression, with no evident damage to treated tissues, thus making it a suitable approach for gene therapy.

Acknowledgments

This research was supported by grants from the California Institute for Regenerative Medicine (CIRM TR406713) to D.G., NIH RO1CA112356 for K.W.F, Milgrom Family Support Program for the Hebrew University to D.G. and Aharon and Ephraim Katzir Travel Grant to G.S.

References

1. Ginn SL, Alexander IE, Edelstein ML, Abedi MR, Wixon J. Gene therapy clinical trials worldwide to 2012 - an update. The journal of gene medicine. 2013; 15:65–77. [PubMed: 23355455]
2. Baum C, Kustikova O, Modlich U, Li ZX, Fehse B. Mutagenesis and oncogenesis by chromosomal insertion of gene transfer vectors. Hum Gene Ther. 2006; 17:253–263. [PubMed: 16544975]
3. Bessis N, GarciaCozar FJ, Boissier MC. Immune responses to gene therapy vectors: influence on vector function and effector mechanisms. Gene Ther. 2004; 11:S10–S17. [PubMed: 15454952]
4. Waehler R, Russell SJ, Curiel DT. Engineering targeted viral vectors for gene therapy. Nat Rev Genet. 2007; 8:573–587. [PubMed: 17607305]

5. Bouard D, Alazard-Dany N, Cosset FL. Viral vectors: from virology to transgene expression. Brit J Pharmacol. 2009; 157:153–165. [PubMed: 18776913]
6. Mehier-Humbert S, Guy RH. Physical methods for gene transfer: improving the kinetics of gene delivery into cells. Advanced drug delivery reviews. 2005; 57:733–753. [PubMed: 15757758]
7. Wells DJ. Gene therapy progress and prospects: electroporation and other physical methods. Gene Ther. 2004; 11:1363–1369. [PubMed: 15295618]
8. Plank C, Schillinger U, Scherer F, Bergemann C, Remy JS, Krotz F, Anton M, Lausier J, Rosenecker J. The magnetofection method: using magnetic force to enhance gene delivery. Biological chemistry. 2003; 384:737–747. [PubMed: 12817470]
9. Taniyama Y, Tachibana K, Hiraoka K, Aoki M, Yamamoto S, Matsumoto K, Nakamura T, Ogihara T, Kaneda Y, Morishita R. Development of safe and efficient novel nonviral gene transfer using ultrasound: enhancement of transfection efficiency of naked plasmid DNA in skeletal muscle. Gene Ther. 2002; 9:372–380. [PubMed: 11960313]
10. Endoh M, Koibuchi N, Sato M, Morishita R, Kanzaki T, Murata Y, Kaneda Y. Fetal gene transfer by intrauterine injection with microbubble-enhanced ultrasound. Molecular therapy : the journal of the American Society of Gene Therapy. 2002; 5:501– 508. [PubMed: 11991740]
11. Sanches PG, Muhlmeister M, Seip R, Kaijzel E, Lowik C, Bohmer M, Tiemann K, Grull H. Ultrasound-mediated gene delivery of naked plasmid DNA in skeletal muscles: a case for bolus injections. Journal of controlled release : official journal of the Controlled Release Society. 2014; 195:130–137. [PubMed: 24979212]
12. Watanabe Y, Horie S, Funaki Y, Kikuchi Y, Yamazaki H, Ishii K, Mori S, Vassaux G, Kodama T. Delivery of Na/I symporter gene into skeletal muscle using nanobubbles and ultrasound: visualization of gene expression by PET, Journal of nuclear medicine : official publication. Society of Nuclear Medicine. 2010; 51:951–958.
13. Li T, Tachibana K, Kuroki M, Kuroki M. Gene transfer with echo-enhanced contrast agents: comparison between Albunex, Optison, and Levovist in mice--initial results. Radiology. 2003; 229:423–428. [PubMed: 14512507]
14. Lu QL, Liang HD, Partridge T, Blomley MJ. Microbubble ultrasound improves the efficiency of gene transduction in skeletal muscle in vivo with reduced tissue damage. Gene Ther. 2003; 10:396–405. [PubMed: 12601394]
15. Wang X, Liang HD, Dong B, Lu QL, Blomley MJ. Gene transfer with microbubble ultrasound and plasmid DNA into skeletal muscle of mice: comparison between commercially available microbubble contrast agents. Radiology. 2005; 237:224–229. [PubMed: 16081853]
16. Qin S, Caskey CF, Ferrara KW. Ultrasound contrast microbubbles in imaging and therapy: physical principles and engineering. Physics in medicine and biology. 2009; 54:R27–57. [PubMed: 19229096]
17. van Wamel A, Bouakaz A, Bernard B, ten Cate F, de Jong N. Radionuclide tumour therapy with ultrasound contrast microbubbles. Ultrasonics. 2004; 42:903–906. [PubMed: 15047404]
18. De Cock I, Zagato E, Braeckmans K, Luan Y, de Jong N, De Smedt SC, Lentacker I. Ultrasound and microbubble mediated drug delivery: Acoustic pressure as determinant for uptake via membrane pores or endocytosis. J Control Release. 2015; 197:20–28. [PubMed: 25449801]
19. Lum AF, Borden MA, Dayton PA, Kruse DE, Simon SI, Ferrara KW. Ultrasound radiation force enables targeted deposition of model drug carriers loaded on microbubbles. Journal of controlled release : official journal of the Controlled Release Society. 2006; 111:128–134. [PubMed: 16380187]
20. Wu J, Ross JP, Chiu JF. Reparable sonoporation generated by microstreaming. The Journal of the Acoustical Society of America. 2002; 111:1460–1464. [PubMed: 11931323]
21. Kuliszewski MA, Kobulnik J, Lindner JR, Stewart DJ, Leong-Poi H. Vascular gene transfer of SDF-1 promotes endothelial progenitor cell engraftment and enhances angiogenesis in ischemic muscle. Molecular therapy : the journal of the American Society of Gene Therapy. 2011; 19:895–902. [PubMed: 21364544]
22. Liang HD, Tang J, Halliwell M. Sonoporation, drug delivery, and gene therapy, Proceedings of the Institution of Mechanical Engineers. Part H. Journal of engineering in medicine. 2010; 224:343–361. [PubMed: 20349823]

23. Klibanov AL. Microbubble contrast agents: targeted ultrasound imaging and ultrasound-assisted drug-delivery applications. Investigative radiology. 2006; 41:354– 362. [PubMed: 16481920]
24. Kaufmann BA, Lindner JR. Molecular imaging with targeted contrast ultrasound. Current opinion in biotechnology. 2007; 18:11–16. [PubMed: 17241779]
25. Borden MA, Kruse DE, Caskey CF, Zhao S, Dayton PA, Ferrara KW. Influence of lipid shell physicochemical properties on ultrasound-induced microbubble destruction. IEEE transactions on ultrasonics, ferroelectrics, and frequency control. 2005; 52:1992– 2002.
26. Stephens DN, Kruse DE, Ergun AS, Barnes S, Lu XM, Ferrara KW. Efficient array design for sonotherapy. Physics in medicine and biology. 2008; 53:3943–3969. [PubMed: 18591737]
27. Shapiro G, Kallai I, Sheyn D, Tawackoli W, Koh YD, Bae H, Trietel T, Goldbart R, Kost J, Gazit Z, Gazit D, Pelled G. Ultrasound-mediated transgene expression in endogenous stem cells recruited to bone injury sites. Polymers for Advanced Technologies. 2014; 25:525–531.
28. Sheyn D, Kimelman-Bleich N, Pelled G, Zilberman Y, Gazit D, Gazit Z. Ultrasoundbased nonviral gene delivery induces bone formation in vivo. Gene Ther. 2008; 15:257– 266. [PubMed: 18033309]
29. Postema M, van Wamel A, Lancee CT, de Jong N. Ultrasound-induced encapsulated microbubble phenomena. Ultrasound in medicine & biology. 2004; 30:827–840. [PubMed: 15219962]
30. Feril LB Jr, Kondo T, Zhao QL, Ogawa R, Tachibana K, Kudo N, Fujimoto S, Nakamura S. Enhancement of ultrasound-induced apoptosis and cell lysis by echocontrast agents. Ultrasound in medicine & biology. 2003; 29:331–337. [PubMed: 12659921]
31. Yang FY, Lee PY. Efficiency of drug delivery enhanced by acoustic pressure during blood-brain barrier disruption induced by focused ultrasound. International journal of nanomedicine. 2012; 7:2573–2582. [PubMed: 22679368]
32. Arranz A, Ripoll J. Advances in optical imaging for pharmacological studies. Frontiers in pharmacology. 2015; 6:189. [PubMed: 26441646]
33. Khalil AA, Jameson MJ, Broaddus WC, Lin PS, Dever SM, Golding SE, Rosenberg E, Valerie K, Chung TD. The Influence of Hypoxia and pH on Bioluminescence Imaging of Luciferase-Transfected Tumor Cells and Xenografts. International journal of molecular imaging. 2013; 2013:287697. [PubMed: 23936647]
34. Burke CW, Suk JS, Kim AJ, Hsiang YH, Klibanov AL, Hanes J, Price RJ. Markedly enhanced skeletal muscle transfection achieved by the ultrasound-targeted delivery of non-viral gene nanocarriers with microbubbles. Journal of controlled release : official journal of the Controlled Release Society. 2012; 162:414–421. [PubMed: 22800583]
35. Kowalczuk L, Boudinet M, El Sanharawi M, Touchard E, Naud MC, Saied A, Jeanny JC, Behar-Cohen F, Laugier P. In vivo gene transfer into the ocular ciliary muscle mediated by ultrasound and microbubbles. Ultrasound in medicine & biology. 2011; 37:1814–1827. [PubMed: 21963032]
36. Li YS, Davidson E, Reid CN, McHale AP. Optimising ultrasound-mediated gene transfer (sonoporation) in vitro and prolonged expression of a transgene in vivo: potential applications for gene therapy of cancer. Cancer letters. 2009; 273:62–69. [PubMed: 18829156]
37. Nomikou N, Tiwari P, Trehan T, Gulati K, McHale AP. Studies on neutral, cationic and biotinylated cationic microbubbles in enhancing ultrasound-mediated gene delivery in vitro and in vivo. Acta biomaterialia. 2012; 8:1273–1280. [PubMed: 21958669]
38. Guzman HR, Nguyen DX, Khan S, Prausnitz MR. Ultrasound-mediated disruption of cell membranes. I. Quantification of molecular uptake and cell viability. The Journal of the Acoustical Society of America. 2001; 110:588–596. [PubMed: 11508983]
39. Delalande A, Bureau MF, Midoux P, Bouakaz A, Pichon C. Ultrasound-assisted microbubbles gene transfer in tendons for gene therapy. Ultrasonics. 2010; 50:269– 272. [PubMed: 19857885]
40. Sirsi S, Borden M. Microbubble Compositions, Properties and Biomedical Applications. Bubble science engineering and technology. 2009; 1:3–17. [PubMed: 20574549]
41. Dayton PA, Morgan KE, Klibanov AL, Brandenburger GH, Ferrara KW. Optical and acoustical observations of the effects of ultrasound on contrast agents. IEEE transactions on ultrasonics, ferroelectrics, and frequency control. 1999; 46:220–232.

42. Liu Y, Yan J, Prausnitz MR. Can ultrasound enable efficient intracellular uptake of molecules? A retrospective literature review and analysis. Ultrasound in medicine & biology. 2012; 38:876–888. [PubMed: 22425381]

43. Liao AH, Hsieh YL, Ho HC, Chen HK, Lin YC, Shih CP, Chen HC, Kuo CY, Lu YJ, Wang CH. Effects of microbubble size on ultrasound-mediated gene transfection in auditory cells. BioMed research international. 2014; 2014:840852. [PubMed: 25254216]

44. Qin S, Ferrara KW. The natural frequency of nonlinear oscillation of ultrasound contrast agents in microvessels. Ultrasound in medicine & biology. 2007; 33:1140– 1148. [PubMed: 17478030]

45. Krasovitski B, Kimmel E. Gas bubble pulsation in a semiconfined space subjected to ultrasound. The Journal of the Acoustical Society of America. 2001; 109:891–898. [PubMed: 11303943]

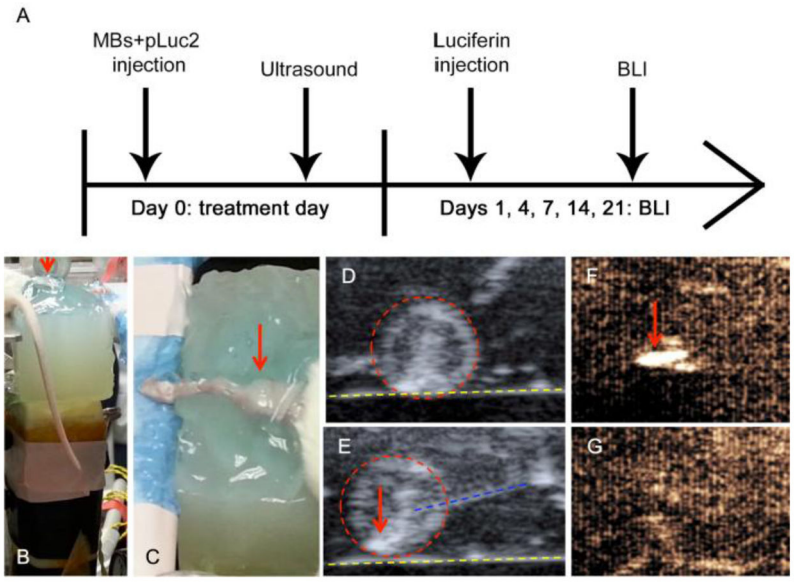

Fig. 1.

Experimental design. A. On Day 0 the mice were injected with a mixture of plasmid DNA (pLuc2) and microbubbles. Immediately after the injection, an ultrasound sequence was applied. Follow-up bioluminescence imaging (BLI) was performed on Days 1, 4, 7, 14, and 21. B and C. On Day 0 ultrasound gel was used to couple the thigh (red arrow) to a spacer on the ultrasound transducer. D and E. With the aid of ultrasound guidance (D, the thigh [marked by a red circle] can be seen on the top of the spacer [marked by a yellow line]), we injected the thigh (E, needle in the thigh [marked by a blue line] can be seen injecting the microbubbles [marked by a red arrow]) with the plasmid DNA – microbubble mix. F and G. During treatment (F, red arrow marks microbubbles) and immediately afterward (G), the injection site was visualized using a contrast-enhanced mode.

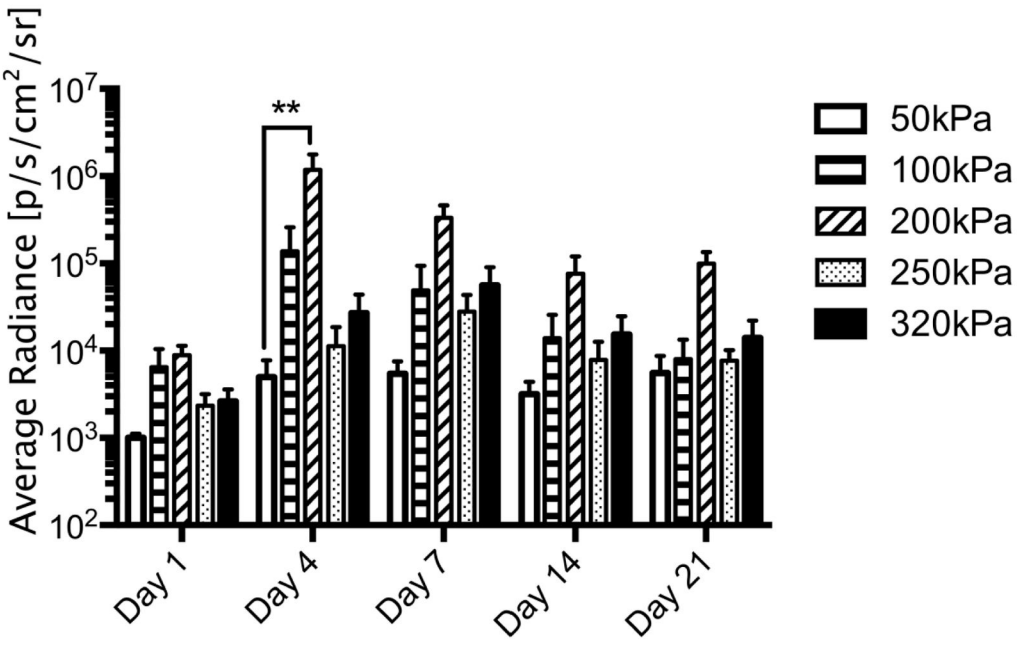

Fig. 2.

Luciferase expression profile in mice treated with microbubble-enhanced sonoporation at various acoustic pressures. Mice were injected once with 50 μg plasmid DNA premixed with 5 x 105 microbubbles and then treated with an acoustic pressure of 50 kPa, 100 kPa, 200 kPa, 250 kPa, or 320 kPa for 2 minutes. The treatment effect was monitored using BLI for 21 days after treatment.

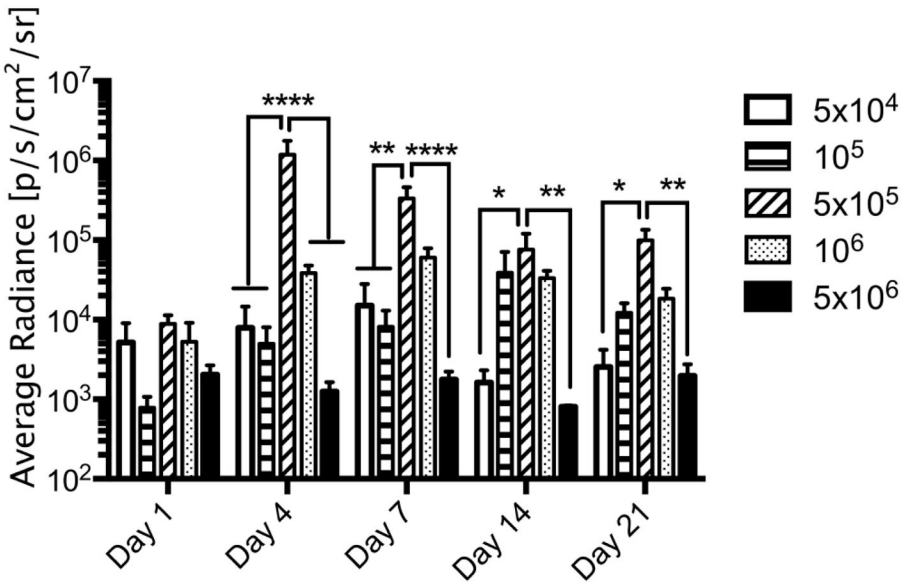

Fig. 3.

Luciferase expression profile in mice treated with microbubble-enhanced sonoporation at various microbubble doses. Mice were injected once with 50 μg plasmid DNA premixed with 5 x 104, 105, 5 x 105, 106, or 5 x 106 microbubbles and then treated with an acoustic pressure of 200 kPa for 2 minutes. The treatment effect was monitored using BLI for 21 days after treatment.

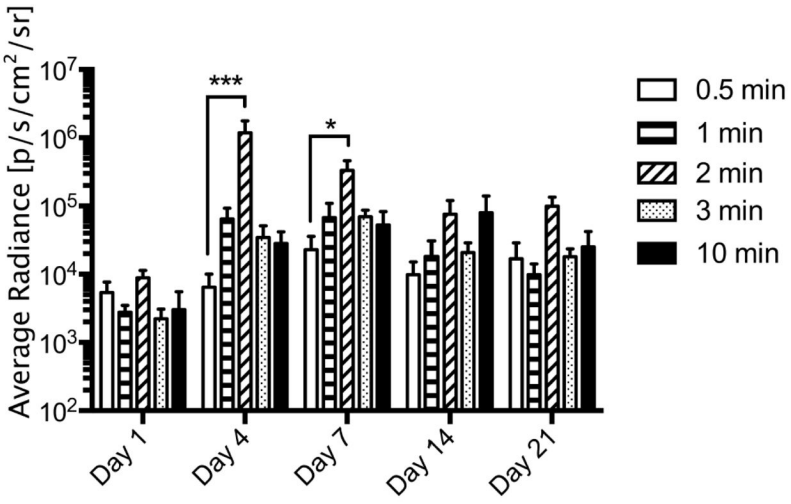

Fig. 4.

Luciferase expression profile in mice treated with microbubble-enhanced sonoporation and with various total treatment times. Mice were injected once with 50 μg plasmid DNA premixed with 5 x 105 microbubbles and then treated with an acoustic pressure of 200 kPa for 0.5 min, 1 min, 2 min, 3 min, or 10 min. The animals. The treatment effect was monitored using BLI for 21 days after treatment.

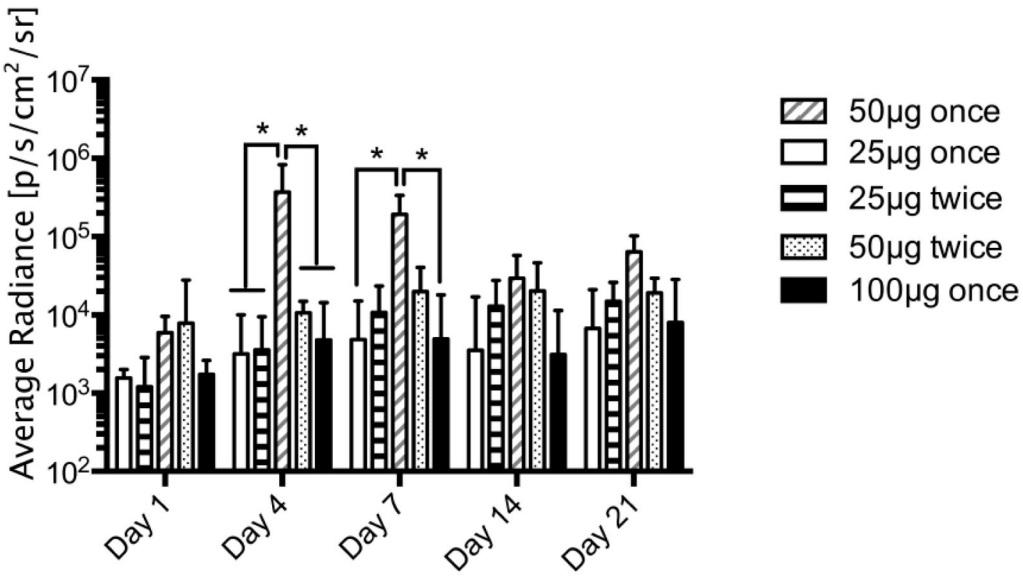

Fig. 5.

Luciferase expression profile in mice treated with microbubble-enhanced sonoporation at various DNA doses and, in some groups, with repeated treatments. Mice were injected once with 25 µg, 50 µg, or 100 µg DNA premixed with 5 x 105 microbubbles and then treated with an acoustic pressure of 200 kPa for 2 min. Other mice were injected with 25 µg or 50 µg DNA premixed with 5 x 105 microbubbles treated with an acoustic pressure of 200 kPa for 2 min and then injected and treated again using the same parameters. The treatment effect was monitored using BLI for 21 days after treatment.

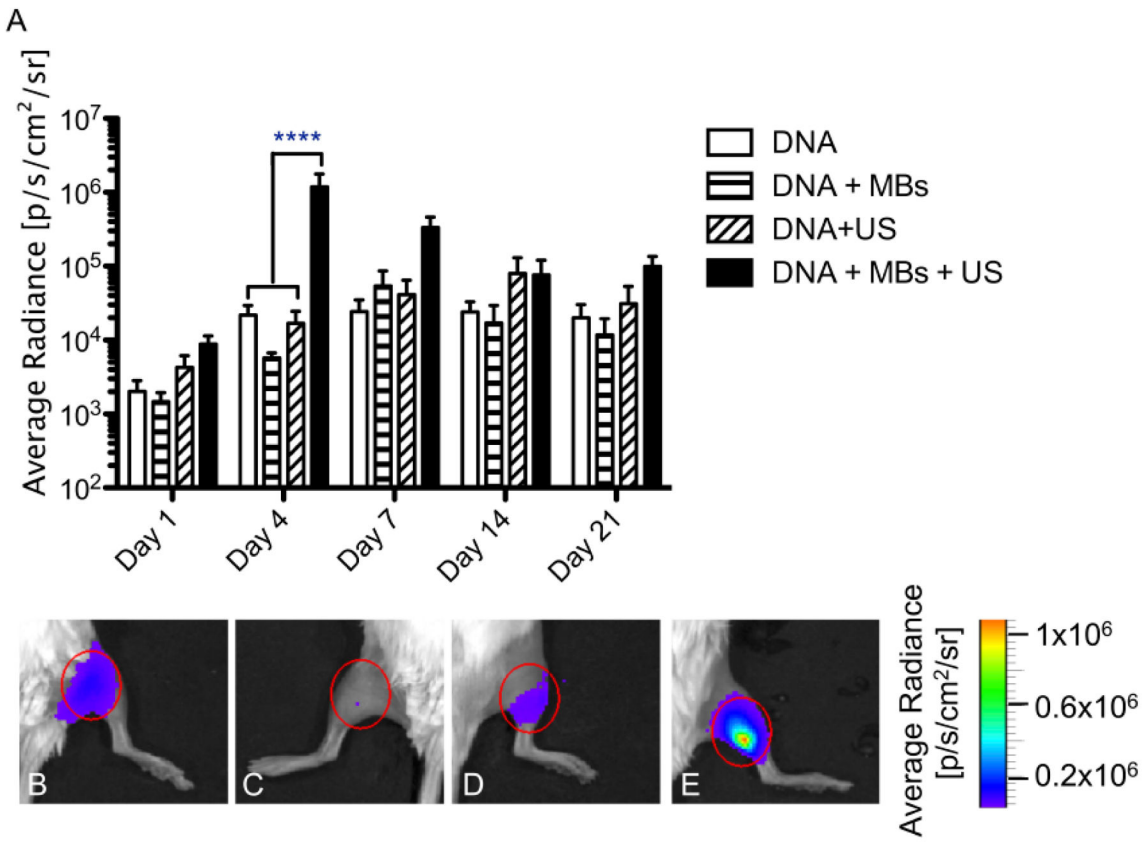

Fig. 6.

A. Luciferase expression profile in mice treated with microbubble-enhanced sonoporation of *Luc2 in vivo*. Mice were injected once with 50 μg plasmid DNA (DNA and DNA + US groups), or 50 μg plasmid DNA premixed with 5 x 105 microbubbles (DNA + MBs and DNA + MBs + US groups) and then treated with an acoustic pressure of 200 kPa for 2 min (DNA + US and DNA + MBs + US group). The treatment effect was monitored using BLI for 21 days after treatment. B. Representative images obtained in each group (respectively in panels B, C, D, and E) on Day 4 with the region of interest indicated by a red oval.

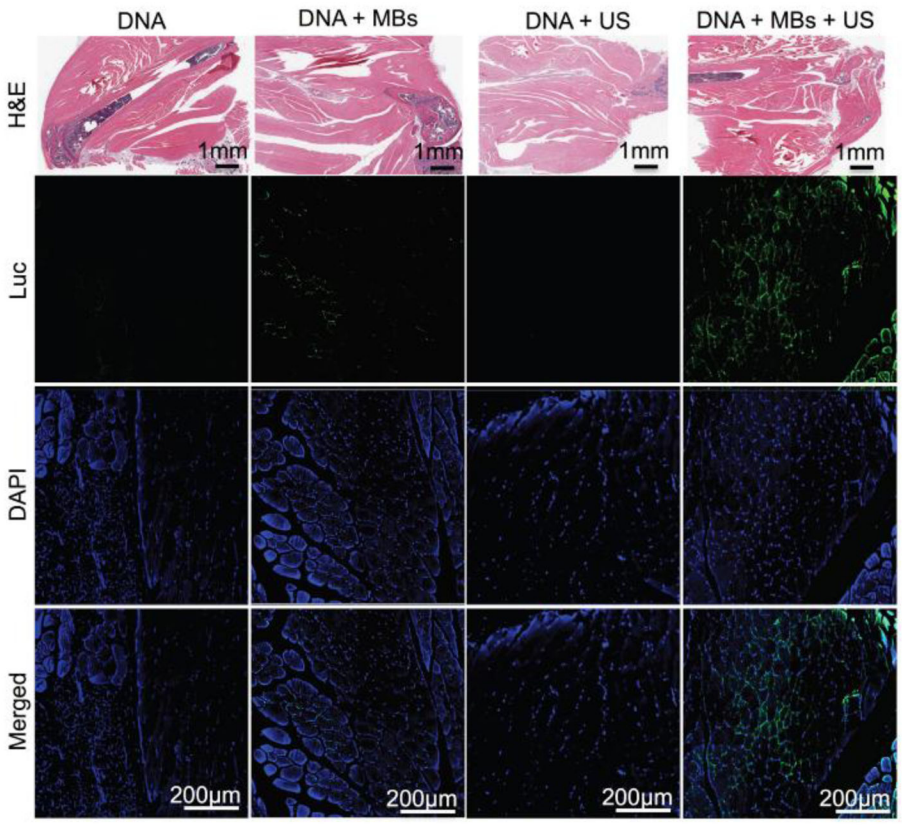

Fig. 7.

In situ luciferase expression induced by microbubble-enhanced sonoporation of *Luc2 in vivo* and detected by immunofluorescent staining. Mice were injected once with 50ug plasmid DNA (DNA and DNA + US groups), or 50ug plasmid DNA premixed with 5 x 105 microbubbles (DNA + MBs and DNA + MBs + US groups) and then treated with an acoustic pressure of 200 kPa for 2 min (DNA + US and DNA + MBs + US group). Thigh muscle sections were treated with H&E or with immunofluorescent staining of luciferase with a DAPI counterstain.

Table 1

Treatment groups. Mice were randomly allocated to 20 treatment groups varying in plasmid DNA dose, MBs dose, acoustic pressure, treatment duration, and number of treatments.

Group	pDNA (μg)	MBs (#/20μl)	Acoustic pressure (kPa)	Treatment duration (min)	Number of treatments
1	50	$5x10^5$	50	2	1
2	50	$5x10^5$	100	2	1
3	50	$5x10^5$	200	2	1
4	50	$5x10^5$	250	2	1
5	50	$5x10^5$	320	2	1
6	50	$5x10^4$	200	2	1
7	50	10^5	200	2	1
8	50	10^6	200	2	1
9	50	$5x10^6$	200	2	1
10	50	$5x10^5$	200	0.5	1
11	50	$5x10^5$	200	1	1
12	50	$5x10^5$	200	3	1
13	50	$5x10^5$	200	10	1
14	25	$5x10^5$	200	2	1
15	25	$5x10^5$	200	2	2
16	50	$5x10^5$	200	2	2
17	100	$5x10^5$	200	2	1
18	50	-	-	-	1
19	50	$5x10^5$	-	-	1
20	50	-	200	2	1